ACS APPLIED MATERIALS & INTERFACES

Research Article

www.acsami.org

# Novel Oligo(ethylene glycol)-Based Molecularly Imprinted Magnetic Nanoparticles for Thermally Modulated Capture and Release of Lysozyme

Nan Li,[†,‡] Li Qi,*[,†] Ying Shen,[†,‡] Juan Qiao,[†] and Yi Chen[†]

[†]Beijing National Laboratory for Molecular Sciences; Key Laboratory of Analytical Chemistry for Living Biosystems, Institute of Chemistry, Chinese Academy of Sciences, Beijing 100190, P. R. China

[‡]Graduate School, University of Chinese Academy of Sciences, Beijing 100049, P. R. China

Supporting Information

**ABSTRACT:** In this study, oligo(ethylene glycol) (OEG)-based thermoresponsive molecularly imprinted polymers (MIPs) for lysozyme on the surface of magnetic nanoparticles were synthesized. Thermoresponsive monomer 2-(2-methoxyethoxy)ethyl methacrylate, chelate monomer *N*-(4-vinyl)-benzyl iminodiacetic acid, and acidic monomer methacrylic acid were selected as the ingredients for preparing the MIP layer. The thermoresponsive behavior of the novel imprinted magnetic nanoparticles was evaluated by dynamic light scattering and swelling ratios measurements. Interestingly, in analysis of lysozyme, the capture/release process could be modulated by changing the temperature, avoiding tedious washing steps. Meanwhile, high adsorption capacity (204.1 mg/g) and good selectivity for capturing lysozyme were achieved. Additionally, surface imprinting with magnetic nanoparticles as substrate allowed for short adsorption time (2 h) and rapid magnetic separation. Furthermore, the proposed imprinted magnetic nanoparticles were used to selectively extract lysozyme in human urine with recoveries ranging from 89.2% to 97.3%. The results indicated that the OEG-based monomers are promising for responsive MIP preparation, and the proposed imprinted material is efficient for thermally modulated capture and release of target protein.

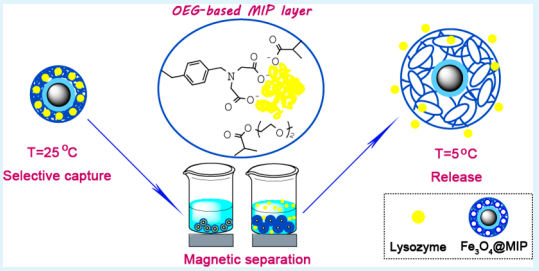


**KEYWORDS:** *oligo(ethylene glycol)-based monomers, thermoresponsive molecularly imprinted polymer, magnetic nanoparticles, surface imprinting, lysozyme*

## 1. INTRODUCTION

Molecular recognition, closely associated with life activity, has attracted considerable attention in research areas including drug delivery, catalysis, immunoassays, and so on.[1] Molecular imprinting is an effective technique to produce specific binding sites for the target molecules in polymer networks. The resultant molecularly imprinted polymers (MIPs) enable the molecular recognition with high specificity and selectivity. Compared with natural receptors, such as antibodies and enzymes, this kind of synthetic receptor possesses the advantages of easy fabrication, reusability, high mechanical/chemical stability, and so on.[2] To date, numerous MIPs for small molecules have been successfully developed for applications in separation, disease diagnosis, sensor, etc.[3−5] However, preparation of MIPs for biomacromolecules, especially proteins, is still a difficult task:[6−8] entrapment of protein molecules in polymer network usually takes place due to their large size, leading to difficulty in removal of protein template; restricted mass transfer leads to the slow kinetics for the capture and release process; the solubility and complex structure of protein cause the weak noncovalent interactions for loading the template, resulting in low adsorption capacity. Despite the challenges, preparation of protein-MIPs has been increasingly attractive because of their great potential in biorelevant applications, especially bioseparation and biopurification.[9]

In the past decades, various approaches for protein imprinting have been developed, such as bulk imprinting, surface imprinting, and epitope imprinting.[10] Among them, surface imprinting, which distributes the binding sites on the substrate surface, is emerging as an outstanding strategy to overcome the restricted mass transfer.[11] As one of the successful examples, Fu and co-workers[6] prepared protein-imprinted nanoparticles via surface graft copolymerization with low monomer concentration. The resultant imprinted material provided dramatically fast kinetics for protein recognition.[7] Moreover, nanomaterials are superior for surface modification because of their extremely large surface area.[8] Among the various nanosized substrates, $Fe_3O_4$ nanoparticles have been widely employed due to their easy preparation and low toxicity. More importantly, they allow for magnetic separation, which can simplify the separation process to a large extent.[12]

**Received:** August 12, 2014
**Accepted:** September 8, 2014
**Published:** September 8, 2014

In addition to the limited mass transfer, difficulty in template removal prevents protein-MIPs from being used in wide applications, especially when the target proteins need to be recovered.[13] Stimuli-responsive materials appear to be an interesting alternative to solve the problem. The combination of the responsive elements with protein-MIPs brings out the so-called responsive protein-MIPs, which can exhibit volume phase transition under the external stimuli (e.g., temperature, pH, and salt). Such intelligent devices provide great possibility to modulate the capture/release process under mild conditions.[14]

Up to date, there have been several thermoresponsive MIPs for proteins; however, they were all constructed on the basis of *N*-isopropylacrylamide (NIPAAm).[15−17] Recently, oligo-(ethylene glycol) (OEG)-based monomers have been emerging as promising alternatives to traditional NIPAAm.[18,19] They are more biocompatible due to the inert ethylene oxide segments. Additionally, phase transition temperatures of OEG-based polymers/hydrogels could be tuned by changing the contents of OEG-based monomers. Moreover, their phase transition temperatures are less affected by other factors (such as molecular weight, ionic strength, concentration, and so on). Considering these advantages, OEG-based monomers are expected to be efficient for preparing biocompatible responsive protein-MIPs with desired phase transition temperatures. However, to our best knowledge, there is no research on employing this kind of monomer into MIP preparation. Lysozyme (Lys) is commonly used as an important indicator for many diseases and a drug for treatment of infections and ulcers.[20] Therefore, developing MIP materials for selective separation of Lys is of great significance.

In this work, an OEG-based thermoresponsive MIP for Lys on the surface of the magnetic nanoparticles was presented. 2-(2-Methoxyethoxy)ethyl methacrylate ($MEO_2MA$), one of the OEG-based thermoresponsive monomers, combined with additional monomers of methacrylic acid (MAA) and *N*-(4-vinyl)-benzyl iminodiacetic acid (VBIDA), was selected to construct the MIP layer. The resulting imprinted nanoparticles were comprehensively characterized. Their thermo-induced swell/shrink behavior was demonstrated by measuring hydrodynamic size and swelling ratios at different temperatures. The binding properties for Lys including adsorption rate, adsorption capacity, and selectivity were investigated. More importantly, thermally modulated capture/release of Lys was carried out by altering the buffer temperature. Furthermore, the prepared imprinted nanoparticles were successfully applied to selectively extract Lys from the synthetic protein mixture in human urine.

## 2. EXPERIMENTAL SECTION

**2.1. Chemicals.** All chemical reagents were directly used as received. Lys (95%), bovine serum albumin (BSA, 98%), cytochrome *c* (Cyt *c*, 98%), pepsin (Pep, 95%), and myoglobin (Mb, 95%) were purchased from Beijing Xin Jing Ke Biotechnology (Beijing, China). *N,N,N′,N′*-Tetramethylethylenediamine (TEMED, 98%) was obtained from MREDA (Beijing, China). 2-(2-Methoxyethoxy)ethyl methacrylate ($MEO_2MA$, 98%), 4-vinylbenzyl chloride (98%), iminodiacetic acid (99%), and γ-methacryloxypropyltrimethoxysilane (MPS, 98%) were purchased from Acros. Ammonium persulfate (APS, ≥99%), *N,N′*-methylenebis(acrylamide) (MBAA, ≥99%), methacrylic acid (MAA, ≥98%), tetraethyl orthosilicate (TEOS, ≥98%), $FeCl_2{\cdot}4H_2O$ (≥99%), and $FeCl_3{\cdot}6H_2O$ (≥99%) were supplied by Beijing Chemical Plant. *N*-(4-Vinyl)-benzyl iminodiacetic acid (VBIDA) was synthesized according to the literature method.[21] Milli-Q water was produced from a water purification system (Millipore). The organic solvents used in the high performance liquid chromatography (HPLC) system were all chromatographic grade. The other unmentioned chemical reagents were analytical grade. Human urine was collected from three healthy volunteers, and 4 mL of each urine sample was concentrated to a solid powder through the freeze-drying method and stored at −4 °C.

**2.2. Instrumentation.** Fourier transform infrared (FTIR) spectra were recorded on a Bruker Tensor-27 spectrophotometer in KBr medium. Elemental analysis was performed with a Flash EA 1112 elemental analyzer (ThermoFinnigan, Milan, Italy). A transmission electron microscopy (TEM) image was obtained from a JEM-2010 high-resolution TEM instrument (JEOL, Japan). Dynamic light scattering (DLS) meaurements were carried out using a BI-90 Plus Particle Size Analyzer (Brookhaven Instruments, USA) with a He−Ne laser ($\lambda$ = 632.8 nm). The scattering angle was set at 173°, and 1 mL of sample (0.001 mg/mL) was filtered through a 0.45 μm film before measurement. Magnetic properties of magnetic nanoparticles were investigated by employing a vibrating sample magnetometer (VSM, LakeShore 7307, USA). UV−vis spectra were recorded using a TU-1900 UV−vis spectrometer (Beijing Purkinje General Instrument, China). HPLC analysis was performed with a Shimadzu LC-20A HPLC system (Shimadzu, Tokyo, Japan), equipped with a personal computer containing a HW-2000 chromatography workstation (Nanjing Qianpu Software, Nanjing, China) and an Agela Technologies Venusil XBP C18 column (Tianjing, China, 5 μm, 100 Å, 4.6 × 150 mm). Water with 0.1 vol % trifluoroacetic acid (TFA) and acetonitrile with 0.1 vol % TFA were used as mobile phases A and B, respectively. The linear gradient profile was as follows: 32.5% A from 0 to 2.8 min, 32.5−36.0% A from 2.8 to 8.0 min, 36.0% A from 8.0 to 11.0 min, and 36.0−80.0% A from 11.0 to 18.0 min.

**2.3. Synthesis of Imprinted and Nonimprinted Magnetic Nanoparticles.** The synthetic scheme for preparing imprinted magnetic nanoparticles is shown in Scheme 1. $Fe_3O_4$ nanoparticles

**Scheme 1. Synthetic Route for Preparing the $Fe_3O_4$@MIP Nanoparticles**

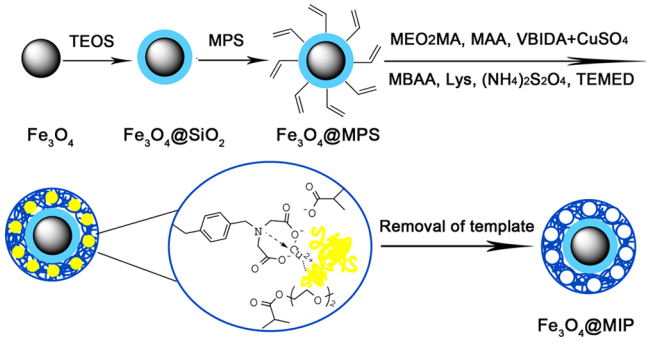


were synthesized by chemical coprecipitation of Fe (III) and Fe (II) according to ref 22. Subsequently, the prepared $Fe_3O_4$ nanoparticles were modified with $SiO_2$ films to afford $Fe_3O_4$@$SiO_2$. Then, $Fe_3O_4$@$SiO_2$ nanoparticles were functionalized with MPS and turned into $Fe_3O_4$@MPS. The detailed procedures were described in the Supporting Information.

MIP layers were modified onto the $Fe_3O_4$@MPS via free radical polymerization. The typical procedure was as follows: $MEO_2MA$ (0.40 mL, 2.167 mmol), VBIDA (0.01 g, 0.040 mmol), $CuSO_4$ (0.01 g, 0.063 mmol), MAA (0.05 mL, 0.470 mmol), MBAA (0.01 g, 0.117 mmol), and 100 mg of Lys were dissolved in 10 mL of phosphate buffer (10 mmol/L, pH = 7.0). Subsequently, 100 mg of $Fe_3O_4$@MPS nanoparticles was added into the above solution. After the mixture was stirred for 2 h, APS (5 mg) and TEMED (5 μL) were added to initiate the polymerization. The reaction was continued for 24 h at room temperature under stirring. Finally, the resultant $Fe_3O_4$@MIP nanoparticles were successively washed with deionized water, NaCl solution (0.2 mol/L), and EDTA solution (0.2 mol/L) until complete removal of the template protein, which was confirmed by UV−vis spectra. The procedure for preparing the nonimprinted magnetic

Table 1. Compositions and Adsorption Capacities ($Q$) of Different Imprinted Magnetic Nanoparticles

| $Fe_3O_4$@MIP | $MEO_2MA$ (mL) | MAA (mL) | VBIDA + $CuSO_4$ (g) | MBAA (g) | Lys (g) | Q (mg/g) |
|---|---|---|---|---|---|---|
| $Fe_3O_4$@MIP1 | 0.40 | 0.05 | 0.01 + 0.01 | 0.01 | 0.05 | 202.85 |
| $Fe_3O_4$@MIP2 | 0.10 | 0.05 | 0.01 + 0.01 | 0.01 | 0.05 | 120.42 |
| $Fe_3O_4$@MIP3 | 0.80 | 0.05 | 0.01 + 0.01 | 0.01 | 0.05 | 108.75 |
| $Fe_3O_4$@MIP4 | 0.40 | 0.00 | 0.01 + 0.01 | 0.01 | 0.05 | 90.37 |
| $Fe_3O_4$@MIP5 | 0.40 | 0.05 | 0.00 + 0.00 | 0.01 | 0.05 | 101.30 |
| $Fe_3O_4$@MIP6 | 0.40 | 0.05 | 0.01 + 0.00 | 0.01 | 0.05 | 140.53 |

nanoparticles ($Fe_3O_4$@NIP) was the same as that for $Fe_3O_4$@MIP except for the absence of Lys in the polymerization mixture.

**2.4. Measurement of Equilibrium Swelling Ratio.** In order to investigate the thermoresponsive properties of the imprinted magnetic nanoparticles, swelling ratios at different temperatures were measured using the gravimetric method. Certain amounts of $Fe_3O_4$@MIP/$Fe_3O_4$@NIP nanoparticles were dried under vacuum to obtain the dry weight ($W_d$). Then, the nanoparticles were incubated in phosphate buffer (10 mmol/L, pH = 7.0) for 12 h at 5, 15, 25, 40, and 50 °C, respectively. After equilibrium, nanoparticles were separated from buffer solution by applying an external magnetic field and the wet weight ($W_w$) was measured. The swelling ratio was calculated as

$$\text{swelling ratio} = \frac{W_w - W_d}{W_d}$$

**2.5. Procedures for Capture and Release of Template Protein.** The typical procedure for capturing protein (template protein and control proteins) was as follows: 5 mg of $Fe_3O_4$@MIP/$Fe_3O_4$@NIP nanoparticles was added to 3 mL of standard protein solution (0.5 mg/mL) prepared in phosphate buffer (10 mmol/L, pH = 7.0). The mixture was stirred for 2 h at room temperature (25 °C). After the capture process completed, the protein concentration in the supernatant was determined by measuring the absorbance at 280 nm. The adsorption capacity ($Q$) of $Fe_3O_4$@MIP/$Fe_3O_4$@NIP was calculated from the following equation:

$$Q = \frac{(c_0 - c)V}{m}$$

where $c_0$ (mg/mL) and $c$ (mg/mL) are the initial protein concentration and final protein concentration in the supernatant, respectively, $V$ (mL) is the volume of buffer solution, and $m$ (mg) is the dry weight of $Fe_3O_4$@MIP/$Fe_3O_4$@NIP nanoparticles in each adsorption solution.

The imprinting factor ($\alpha$) was used to evaluate the specific property of the prepared imprinted nanoparticles, calculated from the following equation:

$$\alpha = \frac{Q_{MIP}}{Q_{NIP}}$$

where $Q_{MIP}$ and $Q_{NIP}$ are adsorption capacity of $Fe_3O_4$@MIP and $Fe_3O_4$@NIP nanoparticles for template protein, respectively.

Thermally modulated capture of Lys was carried out at temperatures ranging from 5 to 50 °C. The adsorption kinetics was studied with adsorption time changed from 0 to 120 min. The adsorption isotherms were studied with Lys concentrations ranging from 0.1 to 2.5 mg/mL. After the adsorption process, the obtained data was linearized using the Langmuir equation as follows:

$$\frac{c_e}{Q} = \frac{c_e}{Q_{max}} + \frac{1}{KQ_{max}}$$

where $K$ (mL/mg) is the dissociation constant for Lys to $Fe_3O_4$@MIP/$Fe_3O_4$@NIP nanoparticles, $c_e$ (mg/mL) is the equilibrium concentration of Lys in solution, and $Q$ (mg/g) and $Q_{max}$ (mg/g) are adsorption capacity and theoretical maximum adsorption capacity, respectively.

For thermally modulated release of Lys, 10 mg of $Fe_3O_4$@MIP/$Fe_3O_4$@NIP nanoparticles was added in 3 mL of 0.5 mg/mL Lys solution, and the mixture was stirred for 2 h at 25 °C. After the Lys molecules were absorbed on the nanoparticles, the supernatant was discarded and 1 mL of phosphate buffer (10 mmol/L, pH = 7.0) containing 0.2 mol/L NaCl was added. The mixture was stirred for 2 h at various temperatures ranging from 5 to 50 °C to release the Lys. The amount of Lys released at each temperature was determined according to the absorbance measured in the UV−vis spectra.

## 3. RESULTS AND DISCUSSION

**3.1. Preparation of Imprinted Magnetic Nanoparticles.** The synthesis of imprinted magnetic nanoparticles exploiting the surface imprinting strategy included modification of silica coatings, functionalization of nanoparticles with vinyl groups, and in situ decoration of the MIP layer. Silica coatings were employed to increase the dispersibility of magnetic nanoparticles and make them more easily encapsulated by polymer layers.[23] The MIP layer was constructed from $MEO_2MA$ combined with additional monomers of MAA and VBIDA. Six kinds of imprinted magnetic nanoparticles differing in monomer compositions were prepared. Their corresponding adsorption capacities for Lys are displayed in Table 1.

$MEO_2MA$ was used as the thermoresponsive component as well as the main functional monomer; therefore, the content of $MEO_2MA$ was vital for achieving efficient thermoresponsive protein-MIP. Compared with $Fe_3O_4$@MIP2 and $Fe_3O_4$@MIP3, $Fe_3O_4$@MIP1 exhibited the best adsorption performance and was thus selected as the optimal one. Effects of MAA and VBIDA were also investigated. It was found that $Fe_3O_4$@MIP4 and $Fe_3O_4$@MIP5, which were prepared in the absence of MAA and VBIDA, respectively, suffered from decreased adsorption capacity. That is because MAA and VBIDA were negatively charged under the polymerization condition (10 mmol/L, pH = 7.0) and could attract Lys through electrostatic interaction. Furthermore, compared with $Fe_3O_4$@MIP6, $Fe_3O_4$@MIP1 prepared in the presence of $Cu^{2+}$ showed much higher adsorption capacity ($Q$), due to VBIDA being able to form a coordinate complex with Lys. The metal coordinate interaction via $Cu^{2+}$ was stronger than the electrostatic interaction directly provided by VBIDA.[24] The increased noncovalent interaction produced the imprinted sites more consistent with the template protein in shape, thus leading to higher adsorption efficiency in the capture process.[25] As expected, the higher imprinting factor ($\alpha$) was also achieved using $Fe_3O_4$@MIP1 because of the more accessible imprinted sites (Figure S1, Supporting Information). The above investigation demonstrated that integrating various interactions for the preparation of imprinted magnetic nanoparticles could greatly enhance the adsorption ability toward the template protein.

Additionally, the effect of $Cu^{2+}$ in the adsorption process was studied. We observed that, as shown in Figure S2, Supporting Information, the values of $Q$ and $\alpha$ were just slightly increased after addition of $Cu^{2+}$. It indicated that the metal coordinate interaction in the adsorption process did not bear a dramatic

improvement in adsorption performance, probably due to the low percentage of VBIDA. Therefore, in order to simplify the operation, all further investigations related to the capture of Lys were carried out using $Fe_3O_4$@MIP1 without $Cu^{2+}$ in the adsorption solution.

**3.2. Characterizations of Imprinted Magnetic Nanoparticles.** Figure 1 exhibits FT-IR spectra of the prepared

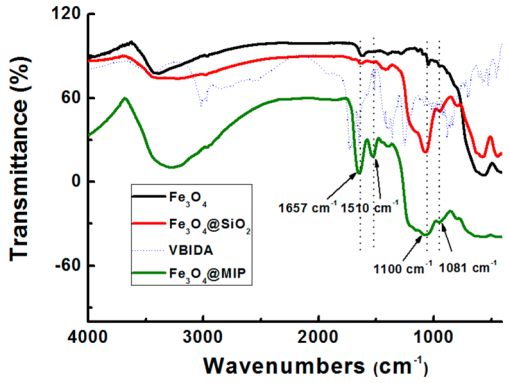


**Figure 1.** FT-IR spectra of bare $Fe_3O_4$ nanoparticles, $Fe_3O_4$@$SiO_2$ nanoparticles, VBIDA, and $Fe_3O_4$@MIP nanoparticles.

magnetic nanoparticles. For $Fe_3O_4$@$SiO_2$ and $Fe_3O_4$@MIP, distinct peaks at 1081 and 1100 $cm^{-1}$ were attributed to the Si−O−Si stretching.[20] In the spectra of $Fe_3O_4$@MIP, the peak at 1510 $cm^{-1}$ was consistent with that of VBIDA and the peak at 1657 $cm^{-1}$ was the characteristic peak of poly($MEO_2MA$).[26] Table 2 displays the results of elemental analysis. After

**Table 2. Elemental Composition of Prepared Magnetic Nanoparticles**

| | elemental composition (wt %) | | |
|---|---|---|---|
| magnetic nanoparticles | C | H | N |
| $Fe_3O_4$ | <0.3 | <0.3 | <0.3 |
| $Fe_3O_4$@$SiO_2$ | <0.3 | <0.3 | <0.3 |
| $Fe_3O_4$@MPS | 1.18 | <0.3 | <0.3 |
| $Fe_3O_4$@MIP | 4.98 | 0.96 | 1.01 |

modification of the MIP layer, contents of carbon, hydrogen, and nitrogen were obviously increased, further demonstrating that the MIP layer has been successfully decorated on the surface of magnetic nanoparticles. It could be observed in the TEM image (Figure S3, Supporting Information) that the prepared $Fe_3O_4$@MIP nanoparticles had a random spherical shape with an average diameter of about 8.6 nm. The morphology and size of the imprinted nanoparticles basically agreed with those prepared by the coprecipitation method.[27]

Magnetic properties of $Fe_3O_4$@MPS and $Fe_3O_4$@MIP were investigated. As exhibited in Figure S4, Supporting Information, magnetization curves were reversible, which was a typical characteristic of superparamagnetism. The saturation magnetization values of $Fe_3O_4$@MPS and $Fe_3O_4$@MIP were 75 and 46 emu/g, respectively. Reduced saturation magnetization for $Fe_3O_4$@MIP is commonly observed because of the increasing number of modification steps.[28] Due to the magnetic characteristic, the imprinted nanoparticles allowed for simple operation and recycling use, which are important for real sample application.

**3.3. Thermoresponsive Properties of Imprinted Magnetic Nanoparticles.** In order to characterize the thermoresponsive property of the OEG-based imprinted magnetic nanoparticles, DLS experiments at various temperatures were carried out. As shown in Figure 2a, we observed

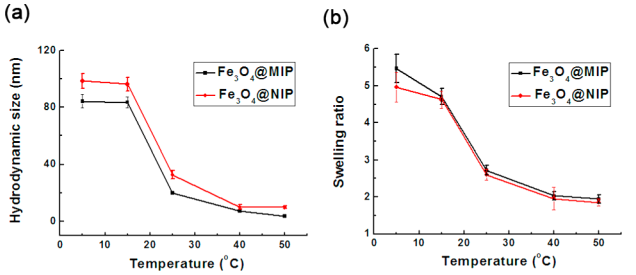


**Figure 2.** (a) Hydrodynamic size and (b) swelling ratios of $Fe_3O_4$@MIP/$Fe_3O_4$@NIP nanoparticles at different temperatures.

that the hydrodynamic size of $Fe_3O_4$@MIP/$Fe_3O_4$@NIP nanoparticles drastically decreased when the temperature increased from 15 to 25 °C. The result indicated that $Fe_3O_4$@MIP/$Fe_3O_4$@NIP nanoparticles had undergone volume phase transitions in this temperature range. Meanwhile, the swelling ratios, which reflected the ability of water loading, were also investigated at different temperatures. As displayed in Figure 2b, the swelling ratio of $Fe_3O_4$@MIP/$Fe_3O_4$@NIP exhibited a significant decrease with temperature increasing from 15 to 25 °C. The reduced water uptake could be explained by the decreased hydrophilicities of the nanoparticles along with the volume phase transitions.[29] All of these results showed that $Fe_3O_4$@MIP/$Fe_3O_4$@NIP exhibited swell/shrink behavior with the change of temperature. Such a stimuli-responsive property is essential for applying the proposed OEG-based imprinted nanoparticles as the temperature switch to modulate the capture and release process.

**3.4. Thermally Modulated Capture of Lys.** The thermoresponsive character was demonstrated, and then, the effect of temperature on Lys capture was investigated. As shown in Figure 3, with an increase in temperature, we observed that the $Q$ value of the $Fe_3O_4$@MIP first increased, reached the maximum at 25 °C, and then slightly decreased. Such thermally modulated capture of Lys was closely related to the swell/shrink behavior of the imprinted nanoparticles. When the temperature was changed from 5 to 25 °C, the imprinted nanoparticles became more hydrophobic. Thus, the strength-

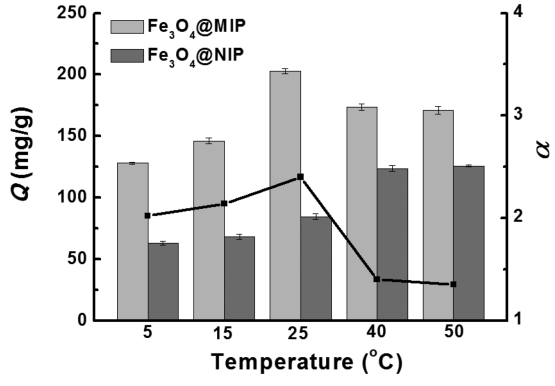


**Figure 3.** Effect of temperature on adsorption capacity ($Q$) of $Fe_3O_4$@MIP/$Fe_3O_4$@NIP nanoparticles and imprinted factor ($\alpha$).

ened hydrophobic interaction between the imprinted nanoparticles and Lys led to a higher $Q$ value. Meanwhile, the imprinted nanoparticles gradually shrunk with the temperature increase. At room temperature (25 °C), the shape of the imprinted cavity was well consistent with that of the template protein, resulting in the best adsorption performance. Further increasing the temperature led to distortions of the imprinted cavities, which made active sites less accessible and thus further decreased the $Q$ value. For $Fe_3O_4$@NIP, the $Q$ value increased along with the increasing temperature in the range of 5−40 °C, which resulted from the increased nonspecific interaction. Additionally, the $\alpha$ value reached the maximum at 25 °C and then sharply decreased, further demonstrating that the capture of Lys above 25 °C was mainly driven by nonspecific adsorption.

**3.5. Adsorption Properties of Imprinted and Nonimprinted Nanoparticles.** At the optimized adsorption temperature, the adsorption properties of $Fe_3O_4$@MIP/$Fe_3O_4$@NIP nanoparticles were investigated. Adsorption kinetics showed that, compared with $Fe_3O_4$@NIP, $Fe_3O_4$@MIP absorbed more Lys because of the stronger specific adsorption (Figure 4a). For both $Fe_3O_4$@MIP and $Fe_3O_4$@

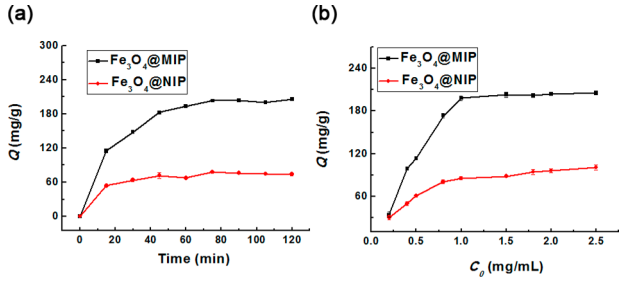


**Figure 4.** (a) Adsorption kinetics and (b) adsorption isotherms of $Fe_3O_4$@MIP/$Fe_3O_4$@NIP nanoparticles.

NIP, the $Q$ value rapidly increased in the first 20 min and then reached equilibrium within only 120 min. The result indicated that the proposed MIP material allowed for a fast adsorption rate, due to a large number of available active sites being located on the surfaces of the magnetic nanoparticles. From the adsorption isotherms (Figure 4b), distinct increases of $Q$ values for $Fe_3O_4$@MIP/$Fe_3O_4$@NIP were found along with an increasing Lys concentration from 0.2 to 1.0 mg/mL. Moreover, the $Q$ values of $Fe_3O_4$@MIP were all higher than those of $Fe_3O_4$@NIP due to the imprinting effect. The experimental data could be well adapted to the Langmuir model to calculate the adsorption parameters. The association constants ($K$) and the maximum adsorption capacity ($Q_{max}$) for $Fe_3O_4$@MIP and $Fe_3O_4$@NIP are shown in Table 3. It could

**Table 3. $K$ and $Q_{max}$ from Langmuir Model**

| samples | $K$ (mL/mg) | $Q_{max}$ (mg/g) |
|---|---|---|
| $Fe_3O_4$@MIP | 4.1 | 204.1 |
| $Fe_3O_4$@NIP | 14.3 | 116.2 |

be found that the $Q_{max}$ value of $Fe_3O_4$@MIP was almost 2 times higher than that of $Fe_3O_4$@NIP, indicating that the imprinted nanoparticles were superior to their nonimprinted counterparts in capturing Lys. Table S1, Supporting Information, lists the adsorption performance (adsorption time, $Q_{max}$, and $K_m$ values) of other reported Lys-MIPs. It has been found that our $Fe_3O_4$@MIP required shorter adsorption time than most of those prepared via both surface imprinting and bulk polymerization. Additionally, it afforded a $Q_{max}$ value 3−18 times higher than those obtained by surface imprinted materials and similar to that of macroporous Lys-imprinted hydrogel.[24] The data demonstrated that the proposed imprinted nanoparticles could achieve a rapid adsorption process and high adsorption capacity simultaneously. Such outstanding adsorption performance made them a promising thermoresponsive device for loading the target protein.

Furthermore, four proteins (Pep, BSA, Cyt $c$, and Mb) differing in molecular weight (MW) and isoelectric point (pI) were used to test the selectivity of the imprinted nanoparticles. As displayed in Figure 5, the proposed imprinted nanoparticles

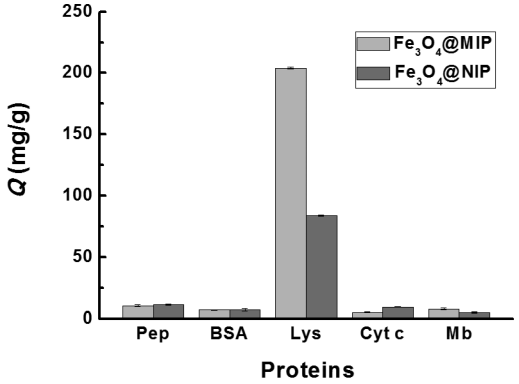


**Figure 5.** $Q$ values of $Fe_3O_4$@MIP and $Fe_3O_4$@NIP nanoparticles for the template protein and the control proteins.

showed high selectivity for Lys. Large proteins, including Pep (pI = 1.0, MW = 35 kDa) and BSA (pI = 4.7, MW = 66.4 kDa), were difficult to capture because the space resistance made them less accessible to magnetic nanoparticles.[30] For electrically neutral protein Mb (pI = 6.8, MW = 16.7 kDa), the low $Q$ value resulted from the absence of the electrostatic interaction in the capture process. The distinct $Q$ value between Lys (pI = 9.3, MW = 14.4 kDa) and Cyt $c$ (pI = 10.7, MW = 12.2 kDa) was explained by the different hydrophobicities of the two proteins. On the basis of the above observations, multiple interactions with the target protein played an important role in the selective capture process.

**3.6. Thermally Modulated Release of Lys.** As shown in Figure 6, it could be observed that the release percentage of Lys

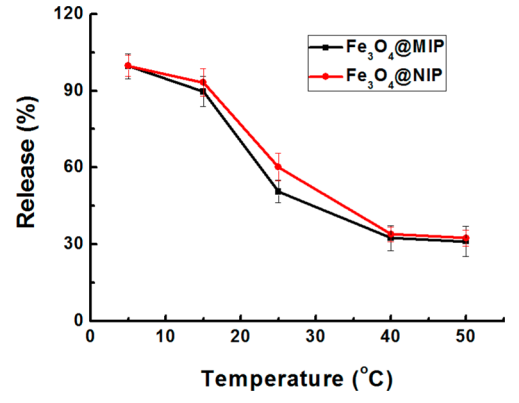


**Figure 6.** Release percentage of $Fe_3O_4$@MIP/$Fe_3O_4$@NIP nanoparticles at different temperatures.

gradually decreased with the increasing temperature. When the temperature increased above 25 °C, only about 30% of absorbed Lys could be released, although 0.2 mol/L NaCl was added to improve the release amount. However, decreasing the temperature to 5 °C led to the almost completed release of Lys under the same condition.

As shown in Figure 7, the phenomenon can be explained by the fact that decreasing temperature made the nanoparticles more hydrophilic and caused swelling. In this process, the interactions between the nanoparticles and Lys were weakened, triggering the release of Lys.[31] Moreover, it has been found that $Fe_3O_4$@MIP nanoparticles released less Lys than $Fe_3O_4$@NIP, probably because of the stronger specific interaction of $Fe_3O_4$@MIP nanoparticles.[32] The results showed that our proposed responsive device allowed for a thermal release process, in which the target protein could be effectively recovered under a mild condition.

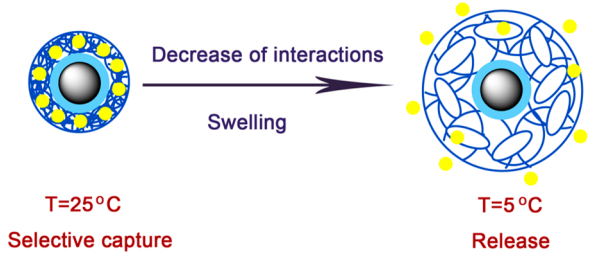


**Figure 7.** Presentation of mechanism for thermally modulated release of Lys.

**3.7. Reusability.** Reusability is an important parameter to evaluate the MIP materials. Figure S5, Supporting Information, represents the adsorption capacities of $Fe_3O_4$@MIP/$Fe_3O_4$@NIP for Lys after the repeated use. The data exhibited that $Fe_3O_4$@MIP/$Fe_3O_4$@NIP allowed for at least 12 cycles of "thermally modulated capture and release" without an obvious decrease of adsorption capacity. The good reusability was attributed to the fact that the release of Lys in this study was achieved by altering the temperature rather than harsh washing with detergents, which usually blocked the active sites and led to poor reusability.[14]

**3.8. Thermally Modulated Capture and Release of Spiked Lys in Human Urine Samples.** In order to evaluate the biological applicability, the prepared $Fe_3O_4$@MIP nanoparticles were further used to extract spiked Lys in three healthy human urine samples. Cyt *c* was added as an interference protein to enhance the complexity of samples. The detailed analytical procedure was described in the Supporting Information. Due to the thermoresponsive property, the target protein could be efficiently captured and released without multiple washing steps. Additionally, separation of the magnetic nanoparticles from solution was achieved under external magnetic fields, avoiding the tedious separation procedure, such as centrifugation. Therefore, a convenient and labor saving process for extracting Lys was carried out. From Figure 8, there was no peak of Lys in the chromatograms of supernatant after being treated with $Fe_3O_4$@MIP nanoparticles, indicating the Lys had been selectively captured. The recoveries of Lys in three human urine samples were shown in Table S2, Supporting Information, and satisfactory recoveries of 89.2–97.3% with acceptable RSD values ranging from 2.7% to 8.1% were obtained. The results indicated that the proposed imprinted nanoparticles were suitable for analysis of Lys in a real sample matrix.

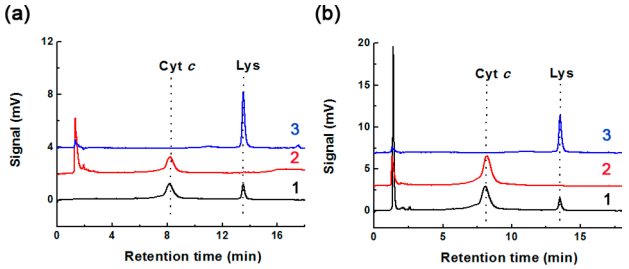


**Figure 8.** HPLC-UV chromatograms of urine samples spiked with (a) 66.7 μg/mL Lys and 66.7 μg/mL Cyt *c* and (b) 66.7 μg/mL Lys and 133.4 μg/mL Cyt *c*. (1) Protein mixture before being treated with $Fe_3O_4$@MIP nanoparticles, (2) protein remaining in supernatant solution after selective recognition, and (3) protein in release solution (In the release process, the volumes of the release solutions were less than those of the capture solution, leading to enhanced signals in chromatograms of Lys).

## 4. CONCLUSION

In this study, OEG-based thermoresponsive imprinted magnetic nanoparticles for Lys were synthesized via surface imprinting. The newly prepared imprinted material has the following advantages: originating from the swell/shrink behavior in response to the temperature change, thermally modulated capture/release of target protein was achieved; through employing mutifunctional monomers, the prepared imprinted nanoparticles exhibited high adsorption capacity and good selectivity; capture of Lys could be completed within short time (2 h); the imprinted magnetic nanoparticles loaded with the target protein can be easily manipulated by the magnetic field. Additionally, they have been successfully used as the temperature switch to selectively extract Lys in human urine samples. Therefore, the proposed imprinted nanoparticles, which are integrated with a thermoresponsive property, magnetic property, and excellent adsorption character, provide a promising alternative for thermally modulated capture/release of target protein.

## ■ ASSOCIATED CONTENT

### Supporting Information

Procedures for preparing $Fe_3O_4$, $Fe_3O_4$@$SiO_2$, and $Fe_3O_4$@MPS, procedure for extraction of lysozyme in human urine samples, effect of copper ions in preparative mixture/adsorption solutions on adsorption capacity of imprinted magnetic nanoparticles, TEM image and magnetic curves, stability test, results of comparing the proposed lysozyme-imprinted material with those reported in the literature, and recoveries of lysozyme in urine samples. This material is available free of charge via the Internet at http://pubs.acs.org.

## ■ AUTHOR INFORMATION

### Corresponding Author

*Tel: +86-10-82627290. Fax: +86-10-62559373. E-mail: qili@iccas.ac.cn.

### Notes

The authors declare no competing financial interest.

## ■ ACKNOWLEDGMENTS

The authors would like to acknowledge financial support from the NSFC (No. 21375132, No. 21175138, No. 21135006, No. 21205125, and No. 21321003).

## ■ REFERENCES

(1) Zhang, H. Water-Compatible Molecularly Imprinted Polymers: Promising Synthetic Substitutes for Biological Receptors. *Polymer* **2014**, *55*, 699−714.
(2) Chen, L.; Xu, S.; Li, J. Recent Advances in Molecular Imprinting Technology: Current Status, Challenges and Highlighted Applications. *Chem. Soc. Rev.* **2011**, *40*, 2922−2942.
(3) Matsui, J.; Akamatsu, K.; Hara, N.; Miyoshi, D.; Nawafune, H.; Tamaki, K.; Sugimoto, N. SPR Sensor Chip for Detection of Small Molecules Using Molecularly Imprinted Polymer with Embedded Gold Nanoparticles. *Anal. Chem.* **2005**, *77*, 4282−4285.
(4) Cheng, Z.; Wang, E.; Yang, X. Capacitive Detection of Glucose Using Molecularly Imprinted Polymers. *Biosens. Bioelectron.* **2001**, *16*, 179−185.
(5) Kempe, M. Antibody-Mimicking Polymers as Chiral Stationary Phases in HPLC. *Anal. Chem.* **1996**, *68*, 1948−1953.
(6) Fu, G.; He, H.; Chai, Z.; Chen, H.; Kong, J.; Wang, Y.; Jiang, Y. Enhanced Lysozyme Imprinting Over Nanoparticles Functionalized with Carboxyl Groups for Noncovalent Template Sorption. *Anal. Chem.* **2011**, *83*, 1431−1436.
(7) He, H.; Fu, G.; Wang, Y.; Chai, Z.; Jiang, Y.; Chen, Z. Imprinting of Protein over Silica Nanoparticles via Surface Graft Copolymerization Using Low Monomer Concentration. *Biosens. Bioelectron.* **2008**, *23*, 1908−1914.
(8) Lin, Z.; Xia, Z.; Zheng, J.; Zheng, D.; Zhang, L.; Yang, H.; Chen, G. Synthesis of Uniformly Sized Molecularly Imprinted Polymer-Coated Silica Nanoparticles for Selective Recognition and Enrichment of Lysozyme. *J. Mater. Chem.* **2012**, *22*, 17914−17917.
(9) Wei, S.; Jakusch, M.; Mizaikoff, B. Capturing Molecules with Templated Materials-Analysis and Rational Design of Molecularly Imprinted Polymers. *Anal. Chim. Acta* **2006**, *578*, 50−58.
(10) Bossi, A.; Bonini, F.; Turner, A. P. F.; Piletsky, S. A. Molecularly Imprinted Polymers for the Recognition of Protein: The State of Art. *Biosens. Bioelectron.* **2007**, *22*, 1131−1137.
(11) Lv, Y.; Tan, T.; Svec, F. Molecular Imprinting of Proteins in Polymers Attached to the Surface of Nanomaterials for Selective Recognition of Biomacromolecules. *Biotechnol. Adv.* **2013**, *31*, 1172−1186.
(12) Aguilar-Arteaga, K.; Rodriguez, J. A.; Barrado, E. Magnetic Solids in Analytical Chemistry: A Review. *Anal. Chim. Acta* **2010**, *674*, 157−165.
(13) Bossi, A.; Piletsky, S. A.; Piletska, E. V.; Righetti, P. G.; Turner, A. P. F. *Anal. Chem.* **2001**, *73*, 5281−5286.
(14) Schirhagl, R. Bioapplications for Molecularly Imprinted Polymers. *Anal. Chem.* **2014**, *86*, 250−261.
(15) Hua, Z.; Chen, Z.; Li, Y.; Zhao, M. Thermosensitive and Salt-Sensitive Molecularly Imprinted Hydrogel for Bovine Serum Albumin. *Langmuir* **2008**, *24*, 5773−5780.
(16) Gai, Q.; Qu, F.; Liu, Z.; Dai, R.; Zhang, Y. Superparamagnetic Lysozyme Surface-Imprinted Polymer Prepared by Atom Transfer Radical Polymerization and Its Application for Protein Separation. *J. Chromatogr., A* **2010**, *1217*, 5035−5042.
(17) Pan, G.; Guo, Q.; Cao, C.; Yang, H.; Li, B. Thermo-Responsive Molecularly Imprinted Nanogels for Specific Recognition and Controlled Release of Proteins. *Soft Matter* **2013**, *9*, 3840−3850.
(18) François, J. F.; Weichenhan, K.; Özgür, A.; Hoth, A. About the Phase Transitions in Aqueous Solutions of Thermoresponsive Copolymers and Hydrogels Based on 2-(2-Methoxyethoxy)ethyl Methacrylate and Oligo(ethylene glycol) Methacrylate. *Macromolecules* **2007**, *40*, 2503−2508.
(19) Lutz, J. F. Polymerization of Oligo(Ethylene Glycol) (Meth)-Acrylates: Toward New Generations of Smart Biocompatible Materials. *J. Polym. Sci., Part A: Polym. Chem.* **2008**, *46*, 3459−3470.
(20) Jing, T.; Du, H.; Dai, Q.; Xia, H.; Niu, J.; Hao, Q.; Mei, S.; Zhou, Y. Magnetic Molecularly Imprinted Nanoparticles for Recognition of Lysozyme. *Biosens. Bioelectron.* **2010**, *26*, 301−306.
(21) Morris, L. R.; Mock, R. A.; Marshall, C. A.; Howe, J. H. Synthesis of Some Amino Acid Derivatives of Styrene. *J. Am. Chem. Soc.* **1959**, *81*, 377−382.
(22) Arya, S.; Solanki, P. R.; Datta, M.; Malhotra, B. D. Recent Advances in Self-Assembled Monolayers Based Biomolecular Electronic Devices. *Biosens. Bioelectron.* **2009**, *24*, 2810−2817.
(23) Deng, Y.; Yang, W.; Wang, C.; Fu, S. A Novel Approach for Preparation of Thermoresponsive Polymer Magnetic Microspheres with Core-Shell Structure. *Adv. Mater.* **2003**, *15*, 1729−1732.
(24) Qin, L.; He, X.; Zhang, W.; Li, W.; Zhang, Y. Macroporous Thermosensitive Imprinted Hydrogel for Recognition of Protein by Metal Coordinate Interaction. *Anal. Chem.* **2009**, *81*, 7206−7216.
(25) Chen, H.; Kong, J.; Yuan, D.; Fu, G. Synthesis of Surface Molecularly Imprinted Nanoparticles for Recognition of Lysozyme Using a Metal Coordination Monomer. *Biosens. Bioelectron.* **2014**, *53*, 5−11.
(26) Ding, J.; Xiao, C.; Tang, Z.; Zhuang, X.; Chen, X. Highly Efficient "Grafting From" an $\alpha$-Helical Polypeptide Backbone by Atom Transfer Radical Polymerization. *Macromol. Biosci.* **2011**, *11*, 192−198.
(27) Shen, Y.; Guo, W.; Qi, L.; Qiao, J.; Wang, F.; Mao, L. Immobilization of Trypsin via Reactive Polymer Grafting from Magnetic Nanoparticles for Microwave-Assisted Digestion. *J. Mater. Chem. B* **2013**, *1*, 2260−2267.
(28) Li, Y.; Ding, M.; Wang, S.; Wang, R.; Wu, X.; Wen, T.; Yuan, L.; Dai, P.; Lin, Y.; Zhou, X. Preparation of Imprinted Polymer at Surface of Magnetic Nanoparticles for the Selective Extraction of Tadalafil from Medicine. *ACS Appl. Mater. Interfaces* **2011**, *3*, 3308−3315.
(29) Bai, S.; Zhang, H.; Sun, J.; Han, J.; Guo, Y. Preparation and pH-Responsive Performance of Silane-Modified Poly(methylacrylic acid). *J. Appl. Polym. Sci.* **2014**, *131*, DOI: 10.1002/app.40403.
(30) Zhang, W.; Qin, L.; He, X.; Li, W.; Zhang, Y. Novel Surface Modified Molecularly Imprinted Polymer Using Acryloyl-$\beta$-cyclodextrin and Acrylamide as Monomers for Selective Recognition of Lysozyme in Aqueous Solution. *J. Chromatogr., A* **2009**, *1216*, 4560−4567.
(31) Yoshimatsu, K.; Lesel, B. K.; Yonamine, Y.; Beierle, J. M.; Hoshino, Y.; Shea, K. J. Temperature-Responsive "Catch and Release" of Proteins by using Multifunctional Polymer-Based Nanoparticles. *Angew. Chem., Int. Ed.* **2012**, *51*, 2405−2408.
(32) Odabaşi, M.; Say, R.; Denizli, A. Molecular Imprinted Particles for Lysozyme Purification. *Mater. Sci. Eng., C* **2007**, *27*, 90−99.